CONF-951007--12
BNL-62351

Dissolution of Sputter-Deposited Iron Oxide Films used as a Model for the Passive Film on Iron

Sannakaisa Virtanen[1)], Patrik Schmuki[1)], Alison J. Davenport and Carissima M. Vitus
Brookhaven National Laboratory, Materials Science Division, Department of Applied Science, Upton, NY 11973

1) On leave from the Swiss Federal Institute of Technology, Institute of Material Chemistry and Corrosion, ETH-Hoenggerberg, 8093 Zurich, Switzerland

ABSTRACT

This paper reports results from XANES (X-ray absorption near edge spectroscopy) studies during polarization of thin sputter-deposited Fe-oxide films in acidic solutions. The dissolution rate of Fe-oxides in acidic solutions was found to be strongly increased by the presence of Fe(2+) in the oxide. During anodic polarization in acidic solutions, a deleterious effect of chloride anions is found compared with sulfates. In HCl solutions of increasing concentration, not only the pH decrease, but also the increasing anion concentration accelerates dissolution. On the other hand, the dissolution rate in sulfuric acid does not depend on the sulfate concentration. During cathodic polarization, the dissolution rate is not affected by the presence of chloride ions. This could be due to the negative surface charge of n-type oxides at potentials lower than the flat-band potential, retarding anion adsorption on the surface. These results suggest that the detrimental role of chloride anions on the stability of Fe oxide films is due to a surface complexation effect. The dissolution rate is fairly independent of the potential in the anodic range, except at very high anodic potentials. The XANES spectra reveal no changes in the average oxide valency during anodic polarization. Thus in the passive range, the dissolution that takes place is mostly chemical rather than electrochemical. The findings and their relevance to the stability of natural passive films are discussed.

INTRODUCTION

In spite of a large amount of work carried out on passivity and stability of passive films, many open questions still exist. Even though many models of the breakdown of passivity are based on the dissolution behaviour of passive films (1), scarce information on the chemical and electrochemical stability of passive films is available. One of the major problems is the that separation of passive film properties from the behavior of the underlying metal or alloy is not a straightforward task. In order to obtain information purely on the properties of passive films, studies on model systems such as synthetic bulk or thin film oxides are necessary. Sugimoto et al. studied the chemical stability of (Fe,Ni and Cr)-oxide films prepared by metalorganic chemical vapor deposition in strong HCl solutions and showed that the corrosion rate is mainly determined by the Cr-content of the mixed oxides (2). Using differently prepared bulk (3) and thin film samples (4), Schmuki et al. have shown that the electronic properties of synthetic Fe- and Cr-oxides are in good agreement with the behaviour of natural passive films on Fe and Cr. Moreover it was

shown that the semiconducting behavior and the chemical stability are determined by the stoichiometry of the oxides.

In the above cited works, the chemical stability of the oxides was studied simply by determining the amount of attack after an exposure of the samples in acidic solutions. In order to reveal information on dissolution mechanisms, more sophisticated methods are needed. In this work, results from in situ XANES (X-ray absorption near edge spectroscopy) studies during electrochemical polarization of sputter-deposited Fe-oxide films in acidic solutions are reported. Using thin film samples, the in-situ XANES technique reveals information on the amount of sample dissolution as well as changes in the valence state of the material (5-8). The dissolution rate obtained from the X-ray data will be compared to the electrochemical behavior. Thus a better understanding of the processes taking place on the oxide surface during anodic polarization can be gained. The nature of reactions taking place on the oxide surface would be difficult to derive from using purely electrochemical methods (e.g. polarization curves), since oxidation of redox species present in the solution can take place in the same potential region as interesting reactions of the oxide itself. Studies on passivated alloys are further complicated by the presence of the underlying material, because the mesaured current density in the passive range can be due to either oxidative dissolution of the passive film or transfer of oxidized metal through the passive film. Studying synthetic oxide films on electrochemically inert substrates provides information purely on the properties of the oxide film.

EXPERIMENTAL

Oxide films were prepared by sputter deposition using Fe_3O_4 and Fe_2O_3 (99.9%) targets. The rf-sputtering system has been previously described in detail in (9). Before each deposition, the sputter chamber was evacuated to a pressure of 4-7 x 10^{-4} Pa. The deposition was carried out in pure Ar (99.998%). The thickness of the sputter-deposited oxide films was determined by performing Rutherford Backscattering Spectroscopy (RBS) and SEM measurements on thick samples and assuming a constant deposition rate as a function of time. The oxide layer thicknesses typically varied between 5 and 60 nm. According to RBS, the chemical composition (Fe/O) ratio of the sputter-deposited layers corresponds approximately to the composition of the target materials. This was also verified by a comparison of high-resolution XANES spectra of the sputter-deposited films with corresponding oxide standards measured in air prior to electrochemical measurements (10).

The oxide films were sputter-deposited on Mylar (6 μm), which had been previously coated by sputter depositing a thin layer of tantalum (200-300 Å) to improve the electrical conductivity of the samples. The cell has been described previously (11), and is one based on Kerkar et al. (12). XANES measurements were carried out in situ during the electrochemical treatment of the samples. The electrolyte solutions were continuously deaerated with a stream of Ar bubbles. This also stirred the solution and removed dissolution products from the vicinity of the electrode. The potentials were measured and are reported against a saturated mercury sulfate reference electrode (MSE, ≈ +0.4 V (SCE)). A platinum wire was used as a counter electrode. The solutions were prepared from reagent grade chemicals and distilled water (Millipore Q, 18 mΩ).

XANES measurements were carried out at Beamline X10C at the National Synchrotron Light Source at Brookhaven National Laboratory. A standard two-crystal Si(111) monochromator was used. The energy scale was calibrated by taking the peak in the first derivative of a spectrum from an iron foil to be the position of the Fe K edge at 7112 eV. The monochromator energy was periodically checked and was found to be very stable during the measurements. The acquisition time for one spectrum was approximately 6 min. In situ measurements on the electrochemically controlled samples were made using fluorescence detection with a Canberra 13-element solid-state detector. Further details of the geometry are given in reference 11.

RESULTS

Fig. 1 shows the anodic polarization curves of Fe_3O_4 and Fe_2O_3 sputter-deposited films in deaerated 1 M HCl. Both oxides show a very similar behavior with a comparable passive current density and potential for oxygen evolution. Similarly, a comparison of the two oxides in 1M H_2SO_4 does not reveal any significant differences in their anodic polarization behavior. Further, almost identical passive current densities are found for Fe_2O_3 in 1M HCl and 1M H_2SO_4 (Fig. 2). The anodic polarization curves thus suggest a similar electrochemical behaviour for both oxides in both acidic solutions studied. In order to be able to attribute the anodic current to oxide dissolution and/or redox reactions taking place on the surface, in situ XANES measurements were carried out during potentiostatic polarization of the samples.

Fig. 3 shows XANES spectra for a thin film sample of Fe_3O_4 (3a) and Fe_2O_3 (3b) after various times in 1M HCl at 0 mV MSE. The edge height decreases much faster for the Fe_3O_4 film indicating a higher dissolution rate. Similarly, in situ XANES results of both oxides exposed to 1M H_2SO_4 at 0 mV MSE leads to measurable dissolution of the Fe_3O_4 sample in contrast to the Fe_2O_3 sample, which shows no changes of the spectra after long polarization in this solution. The sample thickness due to loss of material via dissolution was determined from the edge height of the spectra after background subtraction, by assuming the edge height in the first measurement to correspond to the initial known thickness of the sample. This is shown in Figs. 4 and 5 as a function of exposure time. It is evident from these results that a presence of Fe^{2+} in the oxide decreases its stability against dissolution in acids. This effect is even more pronounced when looking at the behavior of ferrous oxide. The ferrous oxide film was prepared by reducing Fe_2O_3 in 0.1M NaOH. It has been shown earlier that this reduction leads to a solid-state conversion into ferrous oxide/hydroxide (10). In Fig. 6 time-variant XANES spectra (b-e) measured for the thus formed film of ferrous oxide in 0.1M H_2SO_4 in 0 mV MSE are shown. The shift of the edge energy to a lower value after reduction of Fe_2O_3 in NaOH (spectra a, b) indicates conversion into a 2-valent oxide. Subsequent exposure of the reduced oxide to 0.1M H_2SO_4 leads to a very fast dissolution. It has to be pointed out that sputter-deposited films of Fe_2O_3 or Fe_3O_4 show practically no attack in 0.1M H_2SO_4.

A comparison of Figs. 4 and 5 indicates that the dissolution rate of Fe-oxides is strongly depending on the type of acid, the dissolution being enhanced in Cl^--containing acidic solution. The dissolution rate was further found to be enhanced with increasing acidity of solution. This is evident from Fig. 7 which shows the average dissolution rate (determined from at least 5 subsequent spectra) of Fe_3O_4 in H_2SO_4 and HCl solutions at 0 mV MSE

with a varying acid concentration. Fig. 7 also clearly demostrates the much higher aggressivity of chloride solutions towards dissolution compared to sulfate solutions.

The role of anions in the anodic dissolution of iron oxides was further studied by measuring XANES spectra in solutions with a constant acidity but an increasing anion concentration. Fig.8 shows the average dissolution rate of Fe_3O_4 during anodic polarization (0 mV MSE) in 1M acidic solutions as a function of anion concentration. The dissolution rate is significantly accelerated with increasing chloride concentration but shows practically no dependence on the sulfate concentration in the solution.

A comparison of the cathodic dissolution behavior of Fe_2O_3 in 1M H_2SO_4 and in 1M HCl is shown in Fig.9. In the figure, the oxide thicknessis plotted as a function of charge during galvanostatic reduction ($i = -2\ \mu A/cm^2$) in both solutions. It is evident that the cathodic dissolution behavior is identical in H_2SO_4 and in HCl solutions. This was also found for Fe_3O_4 and for other acid concentrations (0.1M and 0.5M).

Fig. 10 shows the potential-dependence of the dissolution rate for Fe_3O_4 in 1M H_2SO_4 and for Fe_2O_3 in 1M H_2SO_4 and in 1M HCl. The dissolution rates were determined by stepping the potential in an anodic direction and measuring at least three subsequent spectra at each potential. From the drop of the edge height at each potential, an average dissolution rate can be determined. In all cases apart from high anodic potentials, a fairly constant dissolution rate with a random scatter and thus no straigthforward potential-dependence is found. A comparison of the edge position of the XANES spectra of Fe_2O_3 at different anodic potentials shows practically no energy shift with increasing potential (Fig. 11), indicating that no changes of the average valency of the oxide takes place. This is the case for both 0.1M H_2SO_4 solution where no measurable dissolution takes place (11a) and 1M HCl which shows fairly rapid dissolution and an increase of the dissolution rate at high anodic potentials (11b). Therefore no evidence for dissolution for iron oxide in higher-valent state at high anodci potentials can be found.

DISCUSSION

The dissolution behavior and chemical stability of iron oxides has been widely studied on bulk oxides FeO, Fe_3O_4 and Fe_2O_3 (13,14). Only very few of studies have been concerned with the electrochemistry of the anodic dissolution process (15-18). The behavior of sputter-deposited oxides can differ from the behavior of bulk oxides, since the structure and the stoichiometry of the thin oxide films are not necessarily identical to that of bulk oxides. Nevertheless, similarities exist for both type of oxides. Generally, the chemical dissolution rate of iron oxides is known to increase by increasing acidity of the solution. This can be seen also in the present results on sputter deposited thin Fe-oxide films. Studies on bulk iron oxides have further shown that the nature and concentration of anions present in solutions influence the dissolution rate (14). In accordance with the present study, chloride ions have been shown to lead to a larger rate constant in empirically determined dissolution rate laws than sulfate ions. This influence has been explained to be due to anion complexation of iron cations.

The in situ XANES data demonstrates the importance of oxide composition (i.e. presence of Fe^{2+}) on the dissolution rates in acidic solutions at potentials above the reductive dissolution rate. The significant role of defects in the oxide film on the dissolution

rate in acidic solutions has been shown by Pryor and Evans (19-23). Studying naturally formed passive films on iron which had been chemically separated from the underlying metal, Evans (21) and Mayne and Pryor (24) have found that such films are almost insoluble in 0.1 and 2 N HCl. In these studies the film composition was found to be γ-Fe_2O_3 by electron diffraction methods. On the other hand, studying the dissolution of bulk iron oxides in acidic solutions, Pryor and Evans came to the conclusion that oxide films deficient in oxygen with the respect to the Fe_2O_3 composition are attacked by acids (19,20,22,23). This is in agreement with the results of the present work.

Comparison of the dissolution rates in chloride- and sulfate-containing acidic solutions shows that chloride anions play a special role in the dissolution of iron oxides. In H_2SO_4, no influence of a varying SO_4^{2-} concentration could be found; therefore the dissolution is due to chemical attack by the H^+ ions. On the other hand, the marked enhancement of the dissolution rate with increasing Cl^--concentrations suggests a complexation of the iron cations with Cl^-. Interestingly, the specific effect of chlorides cannot be seen during cathodic reduction treatments. It has been shown in ref. (10), that during galvanostatic reduction of iron oxides in acidic solutions chemical dissolution takes place in addition to reductive dissolution. The finding of the same dissolution kinetics at cathodic potentials in HCl and in H_2SO_4 can be explained by considering the n-type semiconducting nature of iron oxides (3,4).When in contact with an electrolyte, a space-charge layer is formed in the oxide. At potentials below the flat-band potential, a negative surface charge is present and this can repel anions from the surface (25). For sputter-deposited iron oxide films, a flat-band potential of -250 mV SCE ≈ -650 mV MSE in borate buffer, pH 8.4 was found (4). Assuming a pH-dependence of -60 mV / pH, a flat-band potential of ≈-150 mV MSE at pH 0 would result. The galvanostatic reduction takes place in a potential range of -400 to -300 mV MSE in 1M H_2SO_4 and 1M HCl. Thus a negative surface will be present in the oxide and this can be the reason that no dissolution accelerating effect of chlorides was found. The chemical dissolution step during reduction is thus purely due to the presence of protons in the solution.
This finding indicates that adsorption of aggressive anions is the first step in the dissolution of oxide films. A critical potential exists below which the aggressive anion adsorption is retarded or hindered and therefore the occurrence of Cl^--induced attack becomes potential-dependent. This critical potential is determined by the flat-band potential of the semiconducting oxide.

According to data shown above, at anodic potentials corresponding to the passive region of iron and its alloys, the dissolution rate of iron oxides shows little or no potential-dependence. The dissolution of iron oxides in acidic solutions can be either purely chemical as indicated by equations (1) and (2) or oxidative dissolution can take place (e.g. eq. (3)).

$$Fe_2O_3 + 6H^+ = 2Fe^{3+}(aq) + 3H_2O \quad (1)$$
$$Fe_3O_4 + 8H^+ = 2Fe^{3+}(aq) + Fe^{2+}(aq) + 4H_2O \quad (2)$$
$$Fe_3O_4 + 8H^+ = 3Fe^{3+}(aq) + 4H_2O + e^- \quad (3)$$

In addition it has been suggested in literature that a further oxidation of Fe^{3+} into Fe^{4+} (26) or Fe^{6+} (27) species leading to a transpassive dissolution of the oxide film is possible. The formation of soluble FeO_4^{2-} has been suggested to take place in solutions of pH > 13 (27). According to the Pourbaix-diagram of iron, these species should not exist in the pH range

studied in this paper (28). Due to this and since the XANES spectra showed no sign of a change of the average valency of the iron oxides, the dissolution can be described as purely chemical according to above equations (1) and (2). A further indication of chemical dissolution is the fact that the large differences in the dissolution rate between the two oxide types and in different acidic solutions obtained from the XANES data are not reflected in the values of the current densities of the polarization curves in the passive range. The results of this work suggest that the passive current density measured on passivated metals is mainly connected to a field-assisted transfer of the metal ions through the passive film rather than to a potential-dependent dissolution of the passive film. Thus a measurement of the passive current density of passivated alloys gives information on the protective quality of the passive film but not on the stability of the oxide film itself.

The strong increase of the dissolution rate at high anodic potentials could be due to an additional field-assisted transpassive dissolution of the oxide in this potential range. The potential range of the increased oxide dissolution in the case of Fe_3O_4 in 1M H_2SO_4 and Fe_2O_3 in 1M HCl coincides with the potential range of oxygen evolution. Therefore it is possible that the oxygen evolution reaction leads to changes in the solution pH in the vicinity of the sample surface. The increased dissolution rate may at least partially be due to a decreasing surface pH. However, previous findings on transpassive dissolution of metals taking place in the O_2-evolution region suggest that in strong acid solutions, a pH decrease at the metal surface is not of a major importance, especially since the oxygen evolution leads to a strong bubble formation increasing the stirring of the solution in the vicinity of the surface (29). Strong bubble formation can in the case of the sputter-deposited films further lead to a mechanical disbondment of the films from the Ta substrate. Therefore, it is not possible to determine the origin of the increase of the dissolution rate at high anodic potentials. Nevertheless, if transpassive dissolution of the film takes place, the present work suggests that the valency of iron does not change in the transpassive range. This is consistent with data in literature suggesting that in the beginning of the transpassive potential region dissolution yields Fe^{3+} ions which stem from the corrosion of a Fe_2O_3 passive film (30).

The findings of the effect of potential and solution composition on the dissolution rate of synthetic oxide films can have some implications on the understanding of breakdown of passivity, especially on models based on the chemical dissolution of the passive film. Generally, chemical dissolution models claim that chlorides lead to a local thinning of the passive film due to a formation of soluble iron chloride complexes (1,31,32). The aggressive nature of chloride anions leading to pitting corrosion on passive iron can be at least partially due to an enhancement of the dissolution rate of the iron passive film. Since the dissolution rate of iron oxide films is accelerated by an increase of the chloride-concentration, localized film breakdown can take place at surface heterogeneities leading to a fomation of concentrated solutions in occluded cells (e.g. crevices). The existence of a critical potential for pit nucleation can be due to a hindered anion adsorption at potentials below the flat-band potential, due to a presence of a negative surface charge in the oxide. The findings of this work on the dissolution of iron oxide films in aggressive solutions are a clear indication that solution chemistry plays a role on the stability of the passive film, and not only on the dissolution susceptibility of the underlying metal or alloy.

CONCLUSIONS

In situ XANES studies on thin, sputter deposited iron oxide films in acidic solutions during anodic polarization leads to the following conclusions on the stability of iron oxides in acidic solutions:

1. The dissolution rate of thin iron oxide films in acidic solutions is strongly increased by a presence of Fe(2+) in the oxide.
2. A decrease in pH enhances dissolution. In HCl solutions, the dissolution rate is further increased by increasing Cl^--concentration. In H_2SO_4 solutions, the dissolution rate does not depend on the sulfate content of the solution. The specific effect of chlorides is most probably due to a surface complexation of iron cations by chloride anions.
3. In the potential range of cathodic reductive dissolution, no deleterious effect of chlorides compared to sulfates can be found. This could be due to a negative surface charge on the n-type semiconducting oxide at potentials below the flat-band potential. This negative surface charge repels anions from the surface.
4. At potentials above the range of reductive dissolution, the dissolution rate in 1M H_2SO_4 and in 1M HCl is fairly independent of the potential, except at very high anodic potentials. Thus in the potential range corresponding to the passive region of iron and its alloys dissolution is chemical rather than electrochemical.

ACKNOWLEDGEMENTS

One of the authors (SV) would like to thank the Swiss National Science Foundation (Schweizerischer Nationalfonds) for financial support during her stay at the Brookhaven National Laboratory. Further the Institute of Materials Chemistry and Corrosion (IBWK) of ETH-Zurich is acknowledged for the financial support of PS. This work was performed in part under the auspices of the U.S. Department of Energy, Division of Materials Sciences, Office of Basic Energy Science under Contract No. DE-AC02-76CH00016. Measurements were made at the National Synchrotron Light Source, Brookhaven National Laboratory, which is supported by the U.S. Department of Energy, Division of Materials Sciences and Division of Chemical Sciences. We would also like to thank Prof. T. Maentylae, Dr. P. Vuoristo and Mrs. T. Stenberg, Institute of Materials Science at Tampere University of Technology for help in preparation of the sputter deposited samples and R. Lappalainen, Institute of Physics at University of Helsinki for the Rutherford Backscattering measurements.

REFERENCES

1 S. Szklarska-Smialowska, Pitting Corrosion, NACE, Houston, (1986).
2 K. Sugimoto, M. Seto, S. Tanaka, and N. Hara, J. Electrochem. Soc. **140**, 1586 (1993).
3 P. Schmuki, M. Buechler, S. Virtanen, H. Boehni, R. Mueller, and L. J. Gauckler, J. Electrochem. Soc. (in press).
4 S. Virtanen, P. Schmuki, H. Boehni, P. Vuoristo, and T. Maentylae, J. Electrochem. Soc. **142**, 3067 (1995).
5 A. J. Davenport, H. S. Isaacs, G. S. Frankel, A. G. Schrott, C. V. Jahnes, and M. A. Russak, J. Electrochem. Soc. **138**, 337 (1991).

6 A. J. Davenport, H. S. Isaacs, J. A. Bardwell, B. MacDougall, G. S. Frankel, and A. G. Schrott, Corrosion Sci. **35**, 19 (1993).
7 A. J. Davenport, M. Sansone, J. A. Bardwell, A. J. Aldykiewicz Jr., M. Taube, and C. M. Vitus, J. Electrochem. Soc. **141**, L6 (1994).
8 A. J. Davenport, J. A. Bardwell, and C. M. Vitus, J. Electrochem. Soc. **142**, 721 (1995).
9 P. Vuoristo, PhD Thesis, Publication 84, Tampere University of Technology, Tampere, Finland (1991).
10 P. Schmuki, S. Virtanen, A. J. Davenport, and C. M. Vitus, J. Electrochem. Soc. (submitted for publication).
11 A. J. Davenport and M. Sansone, J. Electrochem. Soc. **142**, 725 (1995).
12 M. Kerkar, J. Robinson, and A. J. Forty, Faraday Discuss. Chem. Soc. **89**, 31 (1990).
13 J. W. Diggle, Oxides and Oxide Films, p. p. 281,**Vol. 2**, Ed. J. W. Diggle, Marcel Dekker Inc., New York, (1973).
14 M. A. Blesa, P. J. Morando, and A. E. Regazzoni, Chemical Dissolution of Metal Oxides, CRC Press, Boca Raton, FL (1994).
15 H.-J. Engell, Z. Phys. Chem. **158**, 158 (1956).
16 N. Valverde, Ber. Bunsenges. Phys. Chem. **80**, 333 (1976).
17 S. Haruyama and K. Masamura, Corr. Sci. **18**, 263 (1978).
18 D. S. Mancey, D. W. Shoesmith, J. Lipkowski, A. C. McBride, and J. Noel, J. Electrochem. Soc. **140**, 637 (1993).
19 M. J. Pryor and U. R. Evans, J. Chem. Soc. (1949).
20 M. J. Pryor and U. R. Evans, J. Chem. Soc. 1259 (1950).
21 U. R. Evans, J. Chem. Soc. 1020 (1927).
22 U. R. Evans, J. Chem. Soc. 478 (1930).
23 U. R. Evans, Z. Elektrochem. 1958 (1958).
24 J. E. O. Mayne and M. J. Pryor, J. Chem. Soc. 1831 (1949).
25 P. Schmuki and H. Boehni, Werkstoffe und Korrosion **42**, 203 (1991).
26 B.D. Cahan, C.-F. Chen, J. Electrochem. Soc. **129**, 921 (1982).
27 C. M. Rangel, R. A. Leitao, and I. T. Fonseca, Electrochim. Acta **34**, 255 (1989).
28 M. Pourbaix, Atlas d'equilibres électrochimiques, Gautier-Villars & Vie, Paris, (1963).
29 D. Landolt, Passivity of Metals, Ed. by R.P. Frankenthaler, J. Kruger, The Electrochemical Society Inc., Princeton, NJ 484 (1978).
30 A. D. Romashkan, A. D. Davydov, V. D. Kasheev, and B. N. Kabanov, Elektrokhimiya **10**, 109 (1974).
31 K. E. Heusler and L. Fischer, Werkstoffe und Korrosion **27**, 551 (1976).
32 N. Sato, J. Electrochem.Soc. **129**, 255 (1982).

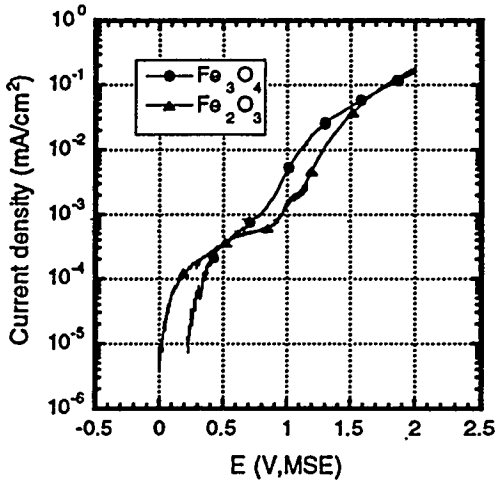

Fig. 1 Anodic polarization curves of sputter-deposited films of Fe_3O_4 and Fe_2O_3 in deaerated 1M HCl (sweep rate 0.5 mV/s).

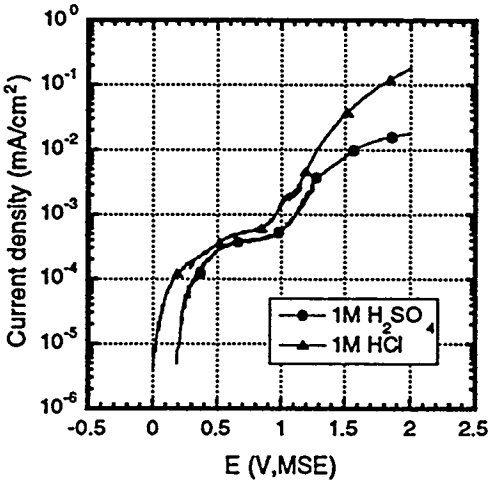

Fig. 2 Anodic polarization curves of sputter-deposited film of Fe_2O_3 in deaerated 1M H_2SO_4 and 1M HCl.
(sweep rate 0.5 mV/s).

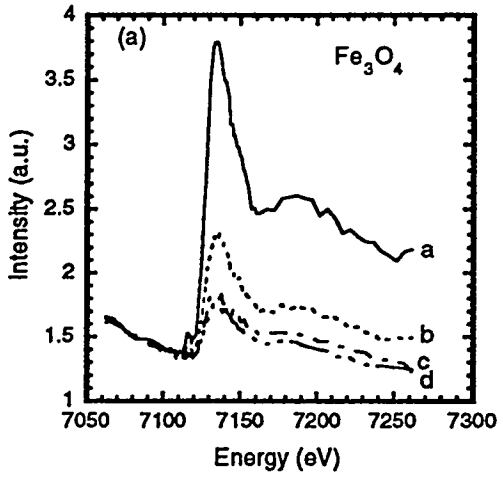

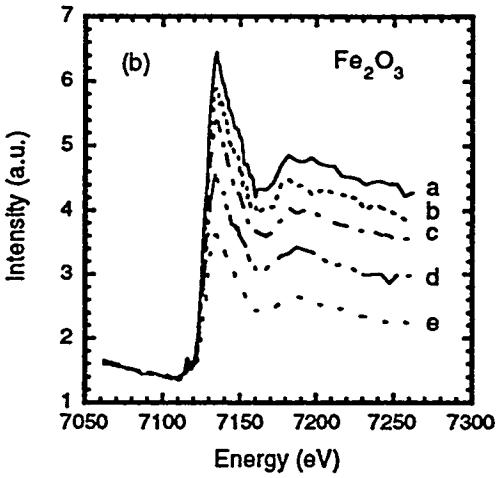

Fig. 3 Consecutive XANES spectra in 1M HCl at 0 mV MSE
a) sputter-deposited film of Fe_3O_4 (d=9.5 nm)
b) sputter-deposited film of Fe_2O_3 (d=9 nm)

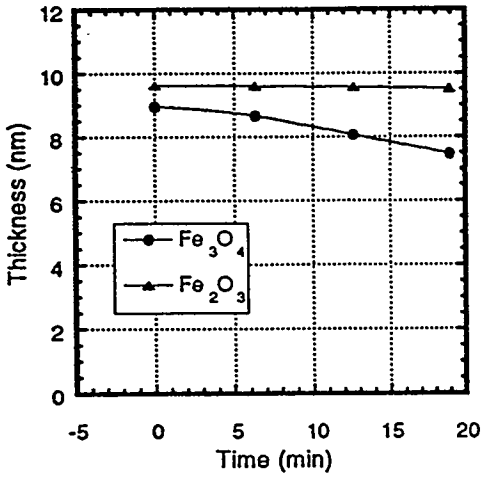

Fig. 4 Thickness of sputter-deposited films of Fe_3O_4 and Fe_2O_3 as a function of exposure time in 1 M H_2SO_4 at 0 mV MSE.

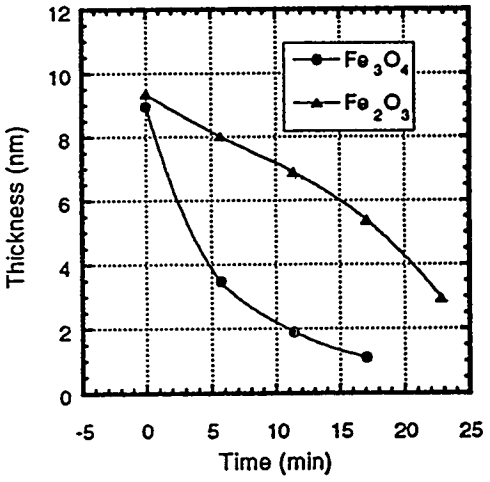

Fig. 5 Thickness of sputter-deposited films of Fe_3O_4 and Fe_2O_3 as a function of exposure time in 1M HCl at 0 mV MSE.

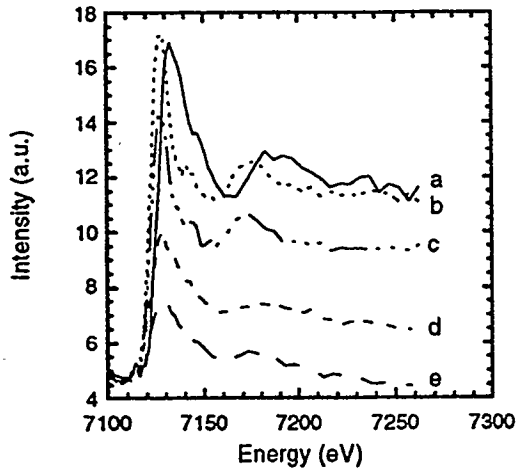

Fig. 6 XANES spectra of a sputter-deposited film of Fe_2O_3 (d=20 nm)
a: as-received film in 0.1M NaOH
b: after galvanostatic reduction (-5μA/cm^2) in 0.1M NaOH
c, d, e: consecutive measurements of the reduced film in 0.1M H_2SO_4 at 0 mV MSE

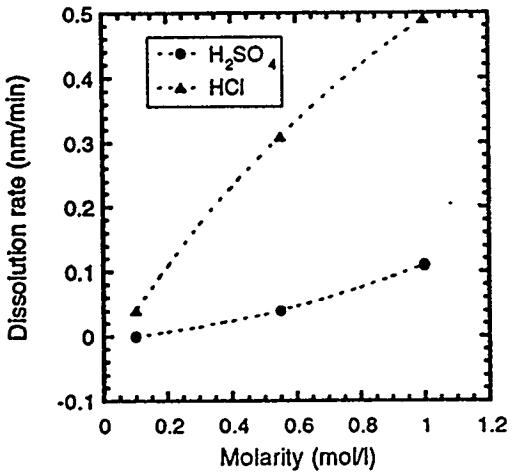

Fig. 7 Dissolution rate of a sputter-deposited film of Fe_3O_4 as a function of acid concentration

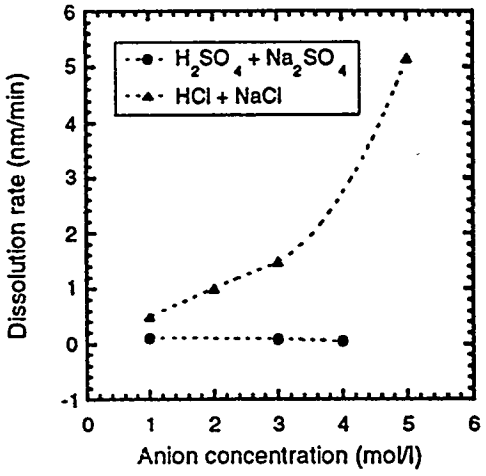

Fig. 8 Dissolution rate of a sputter-deposited film of Fe_3O_4 as a function of anion concentration in 1 M acidic solutions

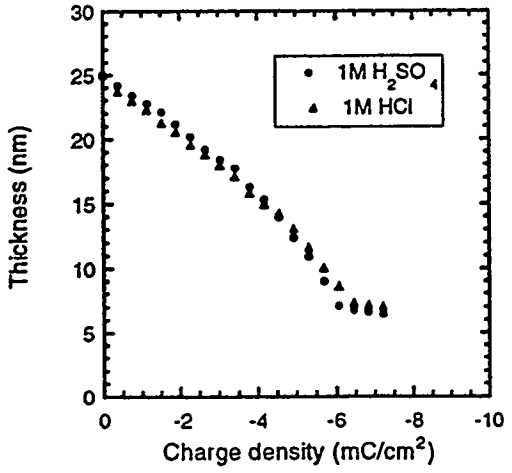

Fig. 9 Thickness of a sputter-deposited film of Fe_2O_3 as a function of reduction charge (galvanostatic reduction with $i = -2\ \mu A/cm^2$) in 1M H_2SO_4 and 1M HCl

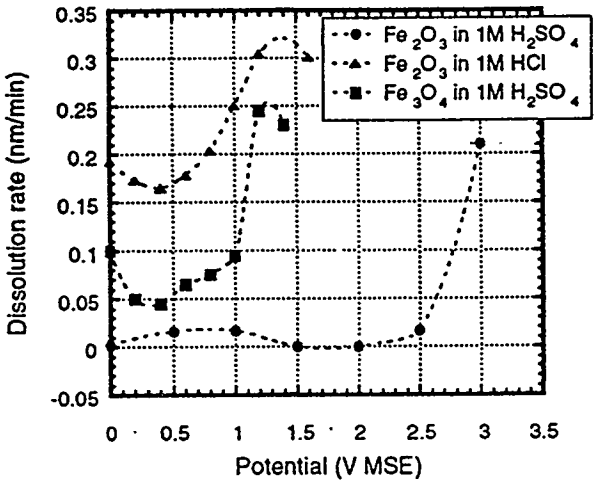

Fig.10 Dissolution rate as a function of potential determined from the decrease of the edge height in XANES spectra during anodic potential steps

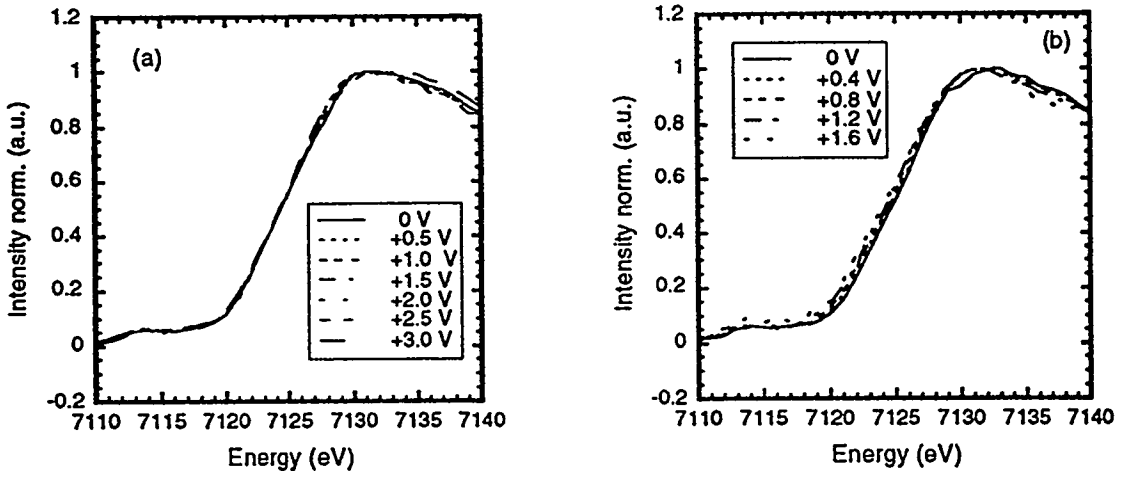

Fig. 11 Normalized XANES for a sputter-deposited film of Fe_2O_3
a) in 0.1M H_2SO_4
b) in 1M HCl